We are IntechOpen,
the world's leading publisher of
Open Access books
Built by scientists, for scientists

**4,800**

Open access books available

**122,000**

International authors and editors

**135M**

Downloads

Our authors are among the

**154**

Countries delivered to

**TOP 1%**

most cited scientists

**12.2%**

Contributors from top 500 universities

CLARIVATE ANALYTICS
**BOOK CITATION INDEX**
INDEXED

**WEB OF SCIENCE™**

Selection of our books indexed in the Book Citation Index
in Web of Science™ Core Collection (BKCI)

Interested in publishing with us?
Contact book.department@intechopen.com

Numbers displayed above are based on latest data collected.
For more information visit www.intechopen.com

# Numerical Analysis of Mixed Convection Magnetohydrodynamic Heat and Mass Transfer past a Stretching Surface in a Micro-Polar Fluid-Saturated Porous Medium Under the Influence of Ohmic Heating

Sandile S. Motsa and Stanford Shateyi

Additional information is available at the end of the chapter

http://dx.doi.org/10.5772/52785

## 1. Introduction

Coupled head and mass transfer by mixed convection in a micro-polar fluid-saturated porous medium due to a stretching sheet has numerous applications in geophysics and energy related engineering problems that engineering problems that includes both metal and polymer sheets. The micro rotation of each particle about its centroid as well as the translatory motion of each particle are taken into account in the study of micro polar fluids.

Past studies on micro polar fluids include, among others, the boundary layer flow of a micro polar fluid over a plate (Rees and Bassom 1996), the flow of a micro polar fluid over a stretching sheet (Raptis,1998) and the flow of a micro polar of fluid in a porons medium (Rawat et al.2007; Motsa et al. 2010; Pal and Chatterjec 2011) .

In many engineering areas processes occur at high temperature so knowledge of radiation heat transfer plays very significant roles and cannot be neglected. Thermal radiation effects become important when the difference between the surface and the ambient temperature is large. Numerous studies have been made to analyze the effect of radiation boundary layer flows under different geometry, (Pal 2009, Pal and Mondal 2010; Shateyi and Motsa 2009; Shateyi and Motsa 2011; Pal and Chatterjec 2011), among others.

In view of the above discussions, we envisage to investigate the steady two-dimensional mixed convection and mass transfer flow past a semi infinite vertical porous plate embedded in a micro polar fluid-saturated porous medium in the presence of thermal radiation, Ohmic dissipation, inertia effects and dispersion effects as these parameters have significant contribution to convective transport process. The problem considered in this chapter has many practical situations such as polymer extrusion processes and the combined effects of the physical parameters will have a large impact on heat and mass transfer characteristics. In this chapter we also aim to solve the current problem using the successive linearization method (Motsa 2011; Motsa and Sibanda 2012) .

## 2. Mathematical formulation

We consider a steady two-dimensional magnetohydrodynamic laminar mixed convection heat and mass transfer flow of a viscous incompressible fluid over a vertical sheet in a micro polar fluid-saturated porous medium. A uniform transverse magnetic field $B_0$ is applied normal to the flow. In this chapter, we assume that the applied magnetic field is taken being weak so that Hall and ion-slip effects maybe neglected. The radiative heat flux in the x-direction is considered negligible in comparison to the y-direction. Under the usual boundary layer approximation, along with Boussinesq's approximations the governing equations describing the conservation of mass, momentum, energy and concentration in the presence of thermal radiation and ohmic heating are governed by the following equations:

$$\frac{\partial u}{\partial x} + \frac{\partial v}{\partial y} = 0, \tag{1}$$

$$u\frac{\partial u}{\partial x} + v\frac{\partial u}{\partial y} = \left(\nu + \frac{k_1^*}{\rho}\right)\frac{\partial^2 u}{\partial y^2} + \frac{k_1^*}{\rho}\frac{\partial N}{\partial y} - \left(\frac{\nu\varphi}{k} + \frac{\sigma B_0^2}{\rho}\right)u - \frac{C_b}{\sqrt{k}}\varphi u^2 + g\beta_t(T - T_\infty)$$
$$+ g\beta_c(C - C_\infty), \tag{2}$$

$$\rho j\left(u\frac{\partial N}{\partial x} + v\frac{\partial N}{\partial y}\right) = \gamma\frac{\partial^2 N}{\partial y^2} - k_1^*(2N + \frac{\partial u}{\partial y}), \tag{3}$$

$$u\frac{\partial T}{\partial x} + v\frac{\partial T}{\partial y} = \frac{1}{\rho c_p}\frac{\partial}{\partial y}\left(\kappa\frac{\partial T}{\partial y}\right) - \frac{1}{\rho c_p}\frac{\partial q_r}{\partial y} + \frac{\delta B_0^2}{\rho c_p}u^2 + \frac{\mu}{\rho c_p}\left(\frac{\partial u}{\partial y}\right)^2, \tag{4}$$

$$u\frac{\partial C}{\partial x} + v\frac{\partial C}{\partial y} = D\frac{\partial^2 C}{\partial y^2}. \tag{5}$$

Where $u, v$ are the velocity components along the $x$- and $y$ - direction, $\rho$ is the density of the fluid, $T$ and $C$ are the temperature and concentration, respectively, $C_b$ is the form of drag coefficient which is independent of viscosity and other properties of the fluid but is dependent on the geometry of the medium, $k$ is the permeability of the porous medium, $\beta_t$ and $\beta_c$ are the coefficients of thermal and concentration expansions, respectively, $\gamma$ is the spin gradient and $k_1^*$ is the vortex viscosity, $c_p$ is the specific heat constant pressure, $\nu$ is the kinematic viscosity, $\sigma$ is the electrical conductivity of the fluid, $B_0$ is externally imposed magnetic field strength, $D$ is the molecular diffusivity , $j$ is the micro inertia per unit mass, $N$ is the component of microrotation or angular velocity whose rotation is in the $x - y$ plane direction. The spin gradient viscosity $\gamma$, defines the relationship between the coefficient of viscosity and micro-inertia as follows (Kim 1999):

$$\gamma = \mu\left(1 + \frac{K}{2}\right)j, \tag{6}$$

with $K = k_1^*/\nu$ being the material parameter. We take $j = \nu/b$ as a reference length. The thermal conductivity $\kappa$ is assumed to vary linearly with temperature and is of the form:

$$\kappa = \kappa_\infty[1 + \epsilon\theta(\eta)], \tag{7}$$

where $\epsilon$ is a small parameter, and following the Rosseland approximation, the radiative heat flux $q_r$ is modeled as,

$$q_r = -\frac{4\sigma^*}{3k^*}\frac{\partial T^4}{\partial y}, \tag{8}$$

where $\sigma^*$ is the Stefan-Boltzmann constant and $k^*$ is the mean absorption coefficient. We assume that the difference in temperature within the flow are such $T^4$ can be expressed as linear combination of the temperature and then $T^4$ can be expanded in Taylor's series about $T_\infty$ as follows:

$$T^4 = T_\infty^4 + 4T_\infty^3(T - T_\infty) + 6T_\infty^2(T - T_\infty)^2 + \ldots\ldots\ldots\ldots \tag{9}$$

Now neglecting higher order terms beyond the first degree in $(T - T_\infty)$ gives

$$T^4 \cong -3T_\infty^4 + 4T_\infty^4 T. \tag{10}$$

Using equations (8) and (10) we obtain

$$\frac{\partial q_r}{\partial y} = -\frac{16T_\infty^3\sigma^*}{3k^*}\frac{\partial^2 T}{\partial y^2}, \tag{11}$$

Using equation (11) in equation (4) gives

$$u\frac{\partial T}{\partial x} + v\frac{\partial T}{\partial y} = \frac{1}{\rho c_p}\frac{\partial}{\partial y}\left(\kappa\frac{\partial T}{\partial y}\right) + \frac{16T_\infty^3\sigma^*}{3k^*}\frac{\partial^2 T}{\partial y^2} + \frac{\delta B_0^2}{\rho c_p}u^2 + \frac{\mu}{\rho c_p}\left(\frac{\partial u}{\partial y}\right)^2, \tag{12}$$

The appropriate boundary conditions for the problem under study are given by:

$$u = u_w = bx, \quad v = 0, \quad N = -n\frac{\partial u}{\partial y} \quad \text{at} \quad y = 0, \quad u \to 0, \quad N \to 0 \quad \text{as} \quad y \to \infty, \tag{13}$$

$$T = T_w = T_\infty + A_0\left(\frac{x}{l}\right)^2, \quad C = C_w = C_\infty + A_1\left(\frac{x}{l}\right)^2, \quad \text{at} \quad y = 0, \tag{14}$$

where $A_0$, $A_1$ are constants, $l$ being the characteristics length, $T_w$ is the wall temperature of the fluid and $T_\infty$ is the ambient fluid temperature, $C_w$ is the wall concentration of the solute and $C_\infty$ is the concentration of the solute far away from the sheet, $n$ is a constant taken as $0 \leq n \leq 1$.

### 2.1. Similarity solutions

In order to reduce the governing equations into a convenient system of ordinary differential equations. We introduce the following self-similar solution of the form:

$$u = bxf'(\eta), \quad v = -\sqrt{bv}f(\eta), \quad \eta = \sqrt{\frac{b}{v}}y, \tag{15}$$

$$N = bx(b/v)^{\frac{1}{2}}g(\eta), \quad \theta(n) = \frac{T - T_\infty}{T_w - T_\infty}, \quad \phi(\eta) = \frac{C - C_\infty}{C_w - C_\infty}, \tag{16}$$

where $f$ is the dimensionless stream function and $\eta$ is the similarity variable. Substituting these into the governing equations, we obtain the following nonlinear ordinary differential equations:

$$(1 + K)f''' + ff'' - (1 + \alpha)f'^2 - \left(M^2 + \frac{1}{Da}\right)f' + Kg' + Gr_t\theta + Gr_m\phi = 0, \tag{17}$$

$$\left(1 + \frac{K}{2}\right)g'' + fg' - f'g - 2Kg - Kf'' = 0, \tag{18}$$

$$\frac{1}{Pr}(1 + R + \epsilon\theta)\theta'' + f\theta' + \frac{\epsilon}{Pr}(\theta')^2 - 2f'\theta + M^2E_c(f')^2 + Ec(f'')^2 = 0, \tag{19}$$

$$\frac{1}{Sc}\phi'' + f\phi' - 2\phi f' = 0, \tag{20}$$

where $\alpha = \frac{C_b}{\sqrt{k}}\varphi x$ is the local inertia coefficient parameter, $\frac{1}{Da} = \frac{\varphi r}{Kb}$ is inverse Darcy number, $M = \sqrt{\frac{\delta}{\rho b}}B_0$ is the Hartmann number, $Gr_t = \frac{g\beta_t(T-T_\infty)}{b^2l}$ is the local Grashof number, $Gr_c = \frac{g\beta_c(C-C_\infty)}{b^2l}$ local concentration Grashof number and $K = k^*/v$ is the material parameter, $Pr = \frac{\mu c_p}{k_\infty}$ is the Prandtl number, $E_c = \frac{b^2l^2}{Ac_p}$ is Ekert number, $R = \frac{16\delta^*T_\infty^3}{3k_\infty k^*}$ is the thermal radiation parameter, $S_c = \frac{v}{D}$ is the Schmidt number. The appropriate boundary conditions 12 and 13 now become:

$$f(\eta) = 0, \quad f'(\eta) = 1, \quad g(\eta) = -nf''(\eta), \quad \theta(\eta) = 1, \quad \phi(\eta) = 1, \text{ at } \eta = 0, \tag{21}$$

$$f'(\eta) \to 0, \quad g(\eta) \to 0, \quad \theta(\eta) \to 0 \quad \phi(\eta) \to 0 \text{ as } \to \infty. \tag{22}$$

## 3. Method of solution

The governing nonlinear problem (16 - 19) is solved using the successive linearization method (SLM). In its basic form, the SLM ([4, 5]) seeks to linearize the governing nonlinear differential equations to a system of linear differential equations which, in most cases, cannot be solved analytically. The Chebyshev pseudospectral method (or any other collocation method or numerical scheme) is then used to transform the iterative sequence of linearized differential equations into a system of linear algebraic equations.

To solve the system of nonlinear equations (16 - 19), we introduce the following notation,

$$(z_1, z_2, z_3, z_4) = (f, g, \theta, \phi) \tag{23}$$

to represent the governing independent variables. In terms of the variables (23), we define the following vector of derivatives of $z_j$ $(j = 1, 2, 3, 4)$, with respect to $\eta$

$$Z_1 = [f, f', f'', f'''] = [z_1^{(0)}, z_1^{(1)}, z_1^{(2)}, z_1^{(3)}], \tag{24}$$

$$Z_2 = [g, g', g''] = [z_2^{(0)}, z_2^{(1)}, z_2^{(2)}], \tag{25}$$

$$Z_3 = [\theta, \theta', \theta''] = [z_3^{(0)}, z_3^{(1)}, z_3^{(2)}], \tag{26}$$

$$Z_4 = [\phi, \phi', \phi''] = [z_4^{(0)}, z_4^{(1)}, z_4^{(2)}]. \tag{27}$$

In general we have

$$Z_i = [z_i^{(0)}, z_i^{(1)}, \ldots, z_i^{(n_i)}], \tag{28}$$

where $z_i^{(0)} = z_i$, $z_i^{(p)}$ is the $p$th derivative of $z_i$ with respect to $\eta$ and $n_i$ $(i = 1, 2, \ldots m)$ is the highest derivative order of the variable $z_i$ appearing in the system of equations. The system (16 - 19) can be written as a sum of it's linear $\mathcal{L}$ and nonlinear components $N$ as

$$\mathcal{L}[z_1(\eta), z_2(\eta), z_3(\eta), z_4(\eta)] + \mathcal{N}[z_1(\eta), z_2(\eta), z_3(\eta), z_4(\eta)] = 0 \tag{29}$$

subject to the boundary conditions

$$A_i[z_1(0), z_2(0), z_3(0), z_m(0)] = K_{a,i}, \quad B_b[z_1(\infty), z_2(\infty), z_3(\infty), z_4(\infty)] = K_{b,i}, \tag{30}$$

where $A_i$ and $B_i$ are linear operators and $K_{a,i}$ and $K_{b,i}$ are constants for $i = 1, 2, \ldots, 4$. In addition, we define $L_i$ and $N_i$ to be the linear and nonlinear operators, respectively, that operate on the $Z_i$ for $i = 1, 2, 3, 4$ With these definitions, equation (29) and (30) can be written as

$$L_i[Z_1, Z_2, Z_3, Z_4] + N_i[Z_1, Z_2, Z_3, Z_4] = \sum_{j=1}^{4} \sum_{p=0}^{n_j} \alpha_{i,j}^{[p]} z_j^{(p)} + N_i[Z_1, Z_2, Z_3, Z_4] = 0 \tag{31}$$

where $\alpha_{i,j}^{[p]}$ are the constant coefficient of $z_j^{(p)}$, the derivative of $z_j$ $(j = 1, 2, 3, 4)$ that appears in the $i$th equation for $i = 1, 2, 3, 4$

The boundary conditions (30) can be written as

$$\sum_{j=1}^{4} \sum_{p=0}^{n_j-1} \beta_{\nu,j}^{[p]} z_j^{(p)}(0) = K_{a,\nu}, \qquad \nu = 1, 2, \ldots, m_a \tag{32}$$

$$\sum_{j=1}^{4} \sum_{p=0}^{n_j-1} \gamma_{\sigma,j}^{[p]} z_j^{(p)}(\infty) = K_{b,\sigma}, \qquad \sigma = 1, 2, \ldots, m_b \tag{33}$$

where $\beta_{\nu,j}^{[p]}$ ($\gamma_{\sigma,j}^{[p]}$) are the constant coefficients of $z_j^{(p)}$ in the boundary conditions, and $m_a$, $m_b$ are the total number of prescribed boundary conditions at $\eta = 0$ and $\eta = \infty$ respectively. We remark that the sum $m_a + m_b$ is equal to the sum of the highest orders of the derivatives corresponding to the dependent variables $z_i$, that is

$$m_a + m_b = \sum_{i=1}^{m} n_i. \tag{34}$$

The SLM assumes that the solution of (29) can be obtained as the convergent series

$$z_i(x) = \sum_{r=0}^{+\infty} z_{i,r}, \tag{35}$$

which, for numerical implementation is truncated at $r = s$ and written as

$$z_i(x) = z_{i,s} + \sum_{r=0}^{s-1} z_{i,r}. \tag{36}$$

A recursive iteration scheme is obtained by substituting (36) into the governing equation (29) and linearizing by neglecting nonlinear terms in $z_{i,s}$ and all it's derivatives. Substituting (36) in (29 - 30) and linearizing gives

$$L_i[Z_{1,s}, Z_{2,s}, Z_{3,s}, Z_{4,s}] + \sum_{j=0}^{4} \sum_{p=0}^{n_j} z_{j,s}^{(p)} \frac{\partial N_i}{\partial z_j^{(p)}}[....] = -L_i[....] - N_i[....], \tag{37}$$

subject to

$$\sum_{j=1}^{4} \sum_{p=0}^{n_j-1} \beta_{\nu,j}^{[p]} z_{j,s}^{(p)}(0) = 0, \qquad \nu = 1, 2, \ldots, m_a \tag{38}$$

$$\sum_{j=1}^{4} \sum_{p=0}^{n_j-1} \gamma_{\sigma,j}^{[p]} z_{j,s}^{(p)}(\infty) = 0, \qquad \sigma = 1, 2, \ldots, m_b \tag{39}$$

where

$$[....] = \left[ \sum_{r=0}^{s-1} Z_{1,r}, \sum_{r=0}^{s-1} Z_{2,r}, \sum_{r=0}^{s-1} Z_{3,r}, \sum_{r=0}^{s-1} Z_{4,r}, \right] \tag{40}$$

The initial approximation $,z_{j,0}(\eta)$, required to start the iteration scheme (37) is chosen to be a function that satisfies the boundary conditions (30). As a guide, the initial guess can be obtained as a solution of the linear part of (29) subject to the boundary conditions (30), that is, we solve

$$\sum_{j=1}^{m} \sum_{p=0}^{n_j} \alpha_{i,j}^{[p]} z_{j,0}^{(p)} = 0 \tag{41}$$

subject to

$$\sum_{j=1}^{4} \sum_{p=0}^{n_j-1} \beta_{v,j}^{[p]} z_{j,0}^{(p)}(0) = K_{a,v}, \qquad v = 1, 2, \ldots, m_a \tag{42}$$

$$\sum_{j=1}^{4} \sum_{p=0}^{n_j-1} \gamma_{\sigma,j}^{[p]} z_{j,0}^{(p)}(\infty) = K_{b,\sigma}, \qquad \sigma = 1, 2, \ldots, m_b \tag{43}$$

To solve the iteration scheme (37), it is convenient to use the Chebyshev spectral collocation method. For brevity, we omit the details of the spectral methods, and refer interested readers to [[12, 13])]. Before applying the spectral method, it is convenient to transform the domain on which the governing equation is defined to the interval [-1,1] on which the spectral method can be implemented. We use the transformation $\eta = \eta_e(\tau + 1)/2$ to map the interval $[0, \eta_e]$ to [-1,1]. Here, it is assumed that $\eta_e$ is a finite real number which is chosen to be large enough to numerically approximate infinity. The basic idea behind the spectral collocation method is the introduction of a differentiation matrix $D$ which is used to approximate the derivatives of the unknown variables $z_i(\eta)$ at the collocation points as the matrix vector product

$$\frac{dz_i}{d\eta} = \sum_{k=0}^{\bar{N}} \mathbf{D}_{lk} z_i(\tau_k) = \mathbf{D}\mathbf{Z}_i, \qquad l = 0, 1, \ldots, \bar{N} \tag{44}$$

where $\bar{N} + 1$ is the number of collocation points (grid points), $\mathbf{D} = 2D/\eta_e$, and $\mathbf{Z} = [z(\tau_0), z(\tau_1), \ldots, z(\tau_N)]^T$ is the vector function at the collocation points. Higher order derivatives are obtained as powers of $\mathbf{D}$, that is

$$z_j^{(p)} = \mathbf{D}^p \mathbf{Z}_j. \tag{45}$$

Applying the Chebyshev spectral collocation on the recursive iteration scheme (37) gives

$$\sum_{j=1}^{m} \left[ \Lambda_{i,j} + \Pi_{i,j} \right] \mathbf{Z}_{j,s} = \Phi_{i,s-1}, \quad i,j = 1,2,3,4 \tag{46}$$

where $\mathbf{Z}_{i,s} = [z_{i,s}(\tau_0), z_{i,s}(\tau_1), \ldots, z_{i,s}(\tau_N)]^T$, $\Lambda_{i,j}$, $\Pi_{i,j}$ and $\Phi_i$ are given by

$$\Lambda_{i,j} = \sum_{p=0}^{n_j} \alpha_{i,j}^p \mathbf{D}^p, \quad \Pi_{i,j} = \sum_{p=0}^{n_j} \frac{\partial N_i}{\partial z_j^{(p)}} \mathbf{D}^p, \quad i,j = 1,2,3,4. \tag{47}$$

and

$$\Phi_{i,s-1} = -L_i[....] - N_i[....], \tag{48}$$

respectively.

Defining $\Delta = \Lambda + \Pi$, we can write equation (46) in matrix form as

$$\begin{bmatrix} \Delta_{1,1} & \Delta_{1,2} & \cdots & \Delta_{1,m} \\ \Delta_{2,1} & \Delta_{2,2} & \cdots & \Delta_{2,m} \\ \vdots & \vdots & & \vdots \\ \Delta_{m,1} & \Delta_{m,2} & \cdots & \Lambda_{m,m} \end{bmatrix} \begin{bmatrix} \mathbf{Z}_{1,s} \\ \mathbf{Z}_{2,s} \\ \mathbf{Z}_{3,s} \\ \mathbf{Z}_{4,s} \end{bmatrix} = \begin{bmatrix} \Phi_{1,s-1} \\ \Phi_{2,s-1} \\ \Phi_{3,s-1} \\ \Phi_{4,s-1} \end{bmatrix} \tag{49}$$

where $\mathbf{Z}_{i,s}$, $\Phi_{i,s-1}$ are vectors of size $(\bar{N}+1) \times 1$ and $\Delta_{i,j}$ are $(\bar{N}+1) \times (\bar{N}+1)$ matrices . After imposing the boundary conditions on the matrix system (49), and starting from $Z_{i,0}$, the recursive sequence (49) is solved iteratively for $s = 1,2,3\ldots$ and the approximate solution for each $z_i(\eta)$ is obtained from the series

$$z_i(\eta) = z_{i,0}(\eta) + z_{i,1}(\eta) + z_{i,2}(\eta) + z_{i,3}(\eta) + \ldots \tag{50}$$

## 4. Results and discussion

This section presents the effects of various parameters on the velocity, temperature, microrotation and concentration profiles. We remark that the, unless otherwise specified, the SLM results presented in this analysis where obtained using $N = 100$ collocation points and $\eta_e = 20$ was used as a numerical approximation infinity. In order to get physical insight into the problem, the effects of these parameters encountered in the governing equations of the problem are analyzed with the help of figures. Figures 1 to 3 depicts effects of the local inertia coefficient parameter $\alpha$, on the velocity, concentration and microrotation distributions. From Figure 1 it is observed that the horizontal velocity profiles decrease with the increasing values of $\alpha$ due to the fact that the second-order quadratic drag is offered by the porous medium to the fluid motion. This drag force results in decreased fluid in the boundary layer. In turn the reduced fluid flow causes the concentration $\phi(\eta)$ to increase as depicted in Figure 2. As expected the increasing values of the local inertia coefficient parameter $\alpha$, causes the gyration component $g(\eta)$ as shown in Figure 3.
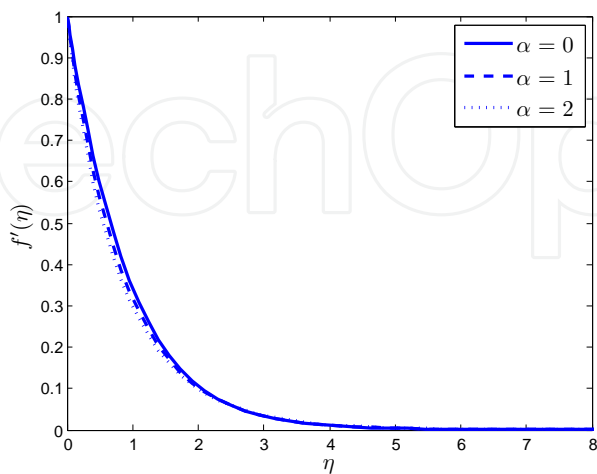
**Figure 1.** Variation of $f'(\eta)$ for different values of $\alpha$ with $K = 0.2; Da = 1; Grt = 1; M = 1; Grm = 1; Pr = 0.71; R = 1; \epsilon = 0.01; Ec = 1; Sc = 1; n = 0.5$.
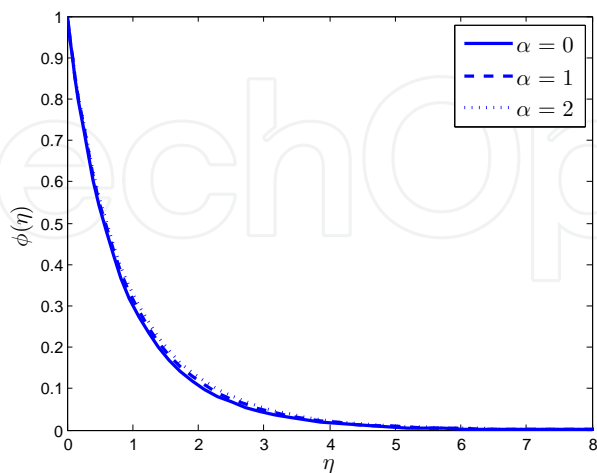


**Figure 2.** Plot of $\phi(\eta)$ for different values of $\alpha$ with $K = 0.2; Da = 1; Grt = 1; M = 1; Grm = 1; Pr = 0.71; R = 1; \epsilon = 0.01; Ec = 1; Sc = 1; n = 0.5$.
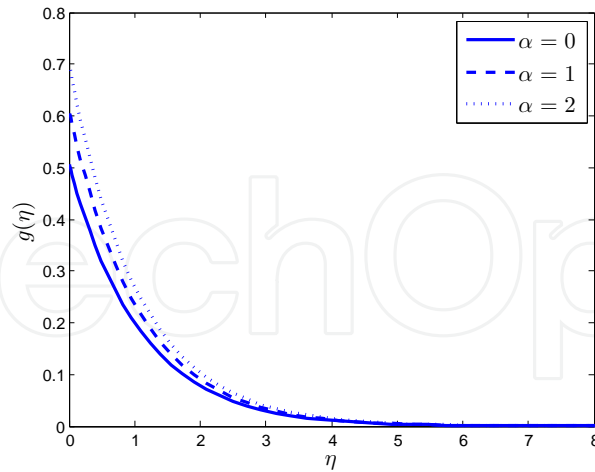
**Figure 3.** Variation of $g(\eta)$ for different values of $\alpha$ with $K = 0.2; Da = 1; Grt = 1; M = 1; Grm = 1; Pr = 0.71; R = 1; \epsilon = 0.01; Ec = 1; Sc = 1; n = 0.5$.

The effects of thermal Grashof number $Gr_t$ on the velocity, temperature, concentration and microrotation distributions are displayed in Figure 4 through Figure 7. From Figure 4 we observe that the horizontal velocity profiles increase with increasing values of the thermal Grashof number $Gr_t$. Buoyancy force acts like a favourable pressure gradient which in turn accelerates the fluid flow within the boundary layer. This accelerated fluid flow leads to the reduction of both the fluid temperature and concentration as can be seen from Figure 5 and Figure 6, respectively. The microrotation profiles are significantly affected by the thermal buoyancy parameter as shown in Figure 7. The increasing values of $Gr_t$ causes the microrotation significantly decrease.
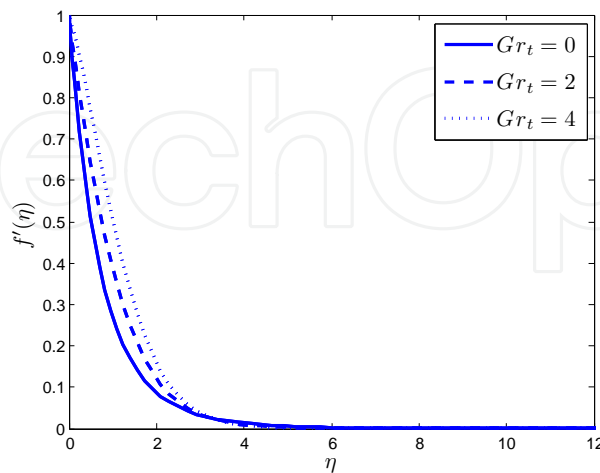


**Figure 4.** The influence of $Gr_t$ on $f'(\eta)$ with $K = 0.2; \alpha = 0.5; Da = 1; Mm = 1; Grm = 1; Pr = 0.71; R = 1; \epsilon = 0.01; Ec = 1; Sc = 1; n = 0.5$.
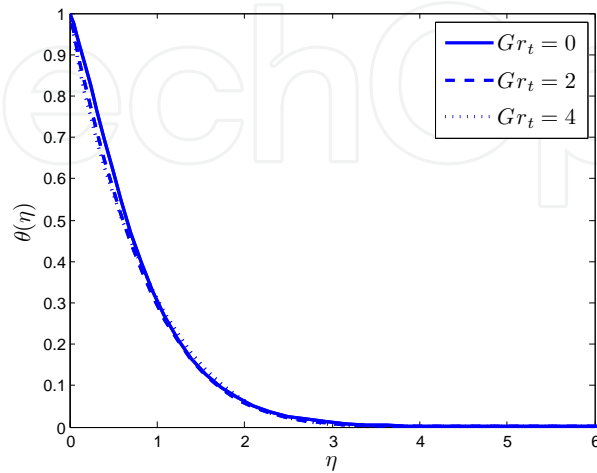
**Figure 5.** Variation of $Gr_t$ on $\theta(\eta)$ when $K = 0.2; \alpha = 0.5; Da = 1; Mm = 1; Grm = 1; Pr = 0.71; R = 1; \epsilon = 0.01; Ec = 1; Sc = 1; n = 0.5$.
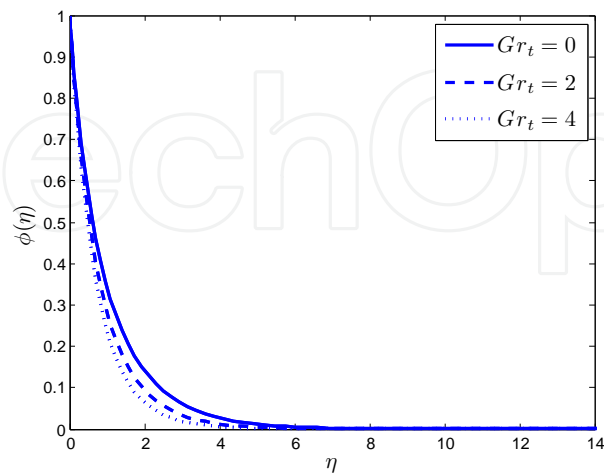


**Figure 6.** $Plot of \phi(\eta)$ for various values of $Gr_t$ when $K = 0.2; \alpha = 0.5; Da = 1; Mm = 1; Grm = 1; Pr = 0.71; R = 1; \epsilon = 0.01; Ec = 1; Sc = 1; n = 0.5$.
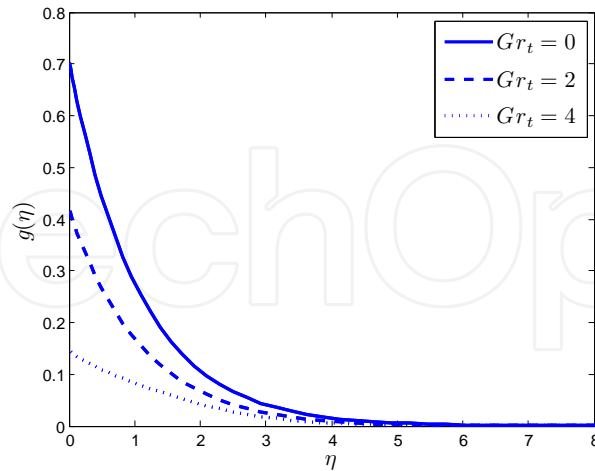
**Figure 7.** Plot of $g(\eta)$ when varying $Gr_t$ with $K = 0.2; \alpha = 0.5; Da = 1; Mm = 1; Grm = 1; Pr = 0.71; R = 1; \epsilon = 0.01; Ec = 1; Sc = 1; n = 0.5$.

Figures 8-11 display results of velocity, temperature, concentration and microrotation distribution for various values of the magnetic parameter $M$. As expected, the existence of the magnetic field is to decrease the velocity in the boundary layer because the application of the transverse magnetic field results in a drag type of force known as Lorentz force. The drag force resists the fluid flow which results in reducing the velocity of the fluid in the boundary layer. The temperature in the boundary layer increases with increasing values of $M$, as shown in Figure 9. From Figure 10, we also observe that the concentration distributions increase as the magnetic parameter $M$ increases. As the magnetic field is applied in the direction of the gyration component, the increasing values of $M$ cause the microrotation distribution to increase as depicted in Figure 11.
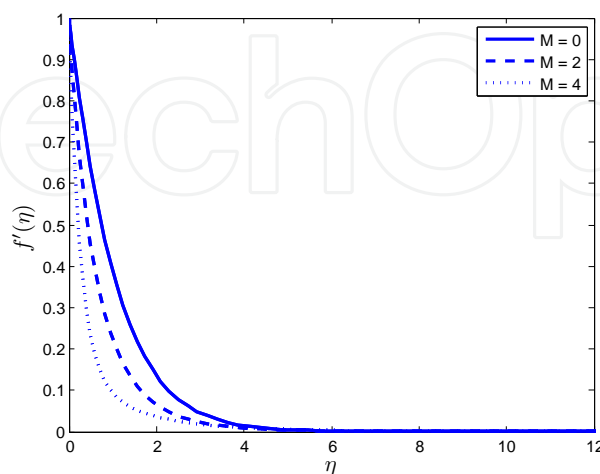


**Figure 8.** The influence of $M$ on $f'(\eta)$ with $K = 0.2; \alpha = 0.5; Da = 1; Grt = 1; Grm = 1; Pr = 5; R = 1; \epsilon = 0.01; Ec = 1; Sc = 1; n = 0.5$.
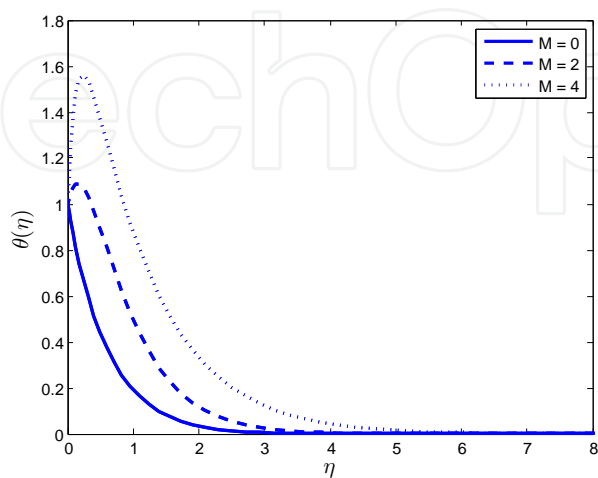
**Figure 9.** Plot of $\theta(\eta)$ for various values of $M$ with $K = 0.2; \alpha = 0.5; Da = 1; Grt = 1; Grm = 1; Pr = 5; R = 1; \epsilon = 0.01; Ec = 1; Sc = 1; n = 0.5$.
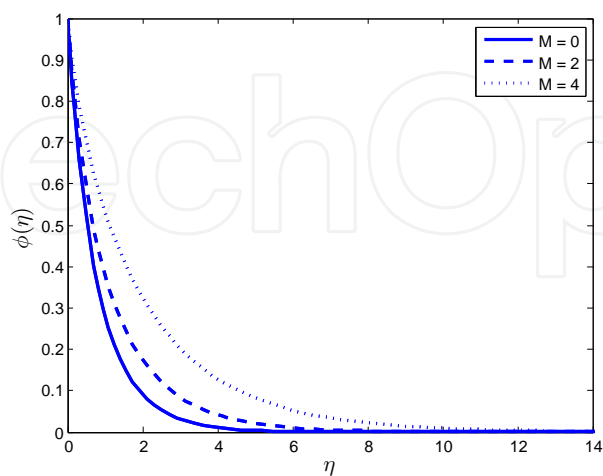


**Figure 10.** Variation of $\phi(\eta)$ for different values of $M$ with $K = 0.2; \alpha = 0.5; Da = 1; Grt = 1; Grm = 1; Pr = 5; R = 1; \epsilon = 0.01; Ec = 1; Sc = 1; n = 0.5$.
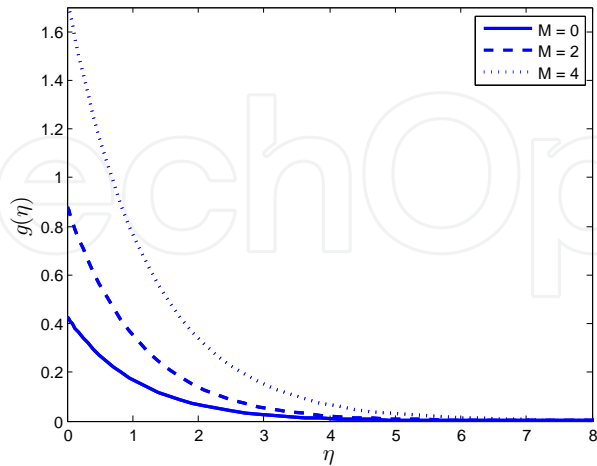
**Figure 11.** Plot of $g(\eta)$ when varying $M$ when $K = 0.2; \alpha = 0.5; Da = 1; Grt = 1; Grm = 1; Pr = 5; R = 1; \epsilon = 0.01; Ec = 1; Sc = 1; n = 0.5$.

The influence of the Darcy number $Da$ on the velocity, temperature, concentration and microrotation profiles is depicted in Figure 12-15. It is clearly observed from these figures that the velocity distribution $f'(\eta)$ increasing with increasing values of the Darcy number $Da$, whereas revers trend is seen on the temperature, concentration and microrotation distributions. This is because the presence of porous medium is to increase the resistance to the flow which causes the fluid flow to decrease.
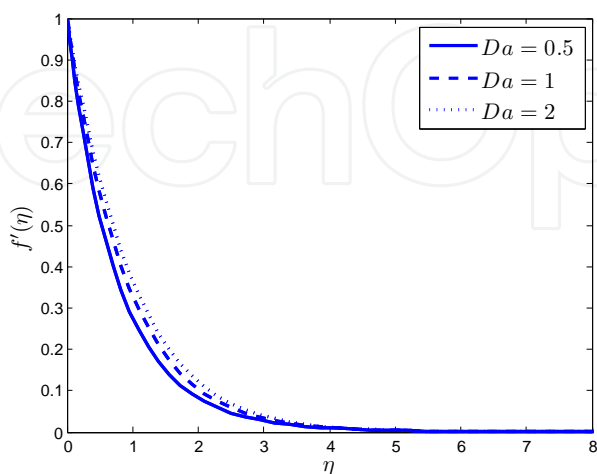


**Figure 12.** Variation of $f'(\eta)$ for different values of $Da$ with $K = 0.2; \alpha = 0.5; Grt = 1; Mm = 1; Grm = 1; Pr = 5; R = 1; e = 0.01; Ec = 1; Sc = 1; n = 0.5$.
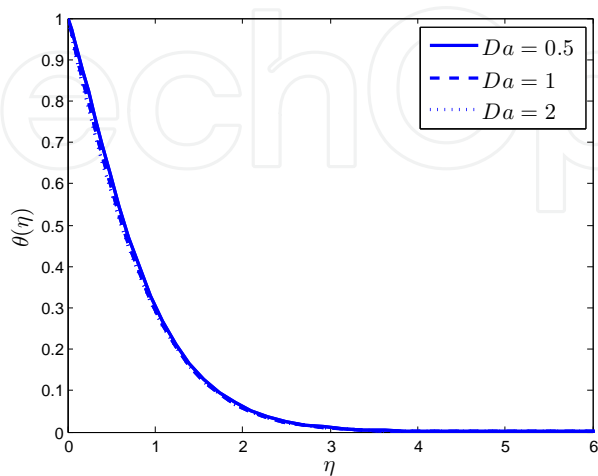
**Figure 13.** Plot of $\theta(\eta)$ for different values of $Da$ $K = 0.2; \alpha = 0.5; Grt = 1; Mm = 1; Grm = 1; Pr = 5; R = 1; e = 0.01; Ec = 1; Sc = 1; n = 0.5$.
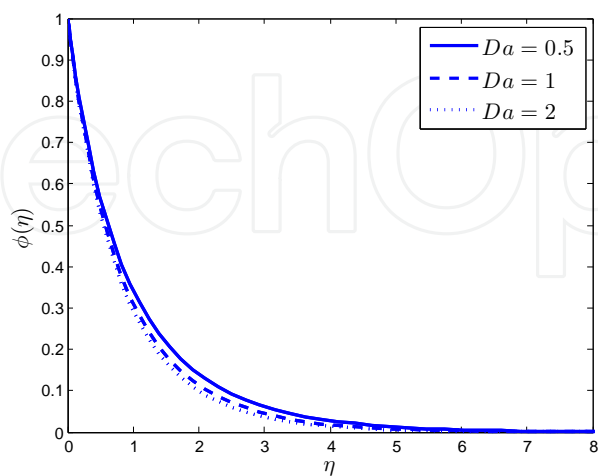


**Figure 14.** Influence of $Da$ on $\phi(\eta)$ when $K = 0.2; \alpha = 0.5; Grt = 1; Mm = 1; Grm = 1; Pr = 5; R = 1; e = 0.01; Ec = 1; Sc = 1; n = 0.5$.
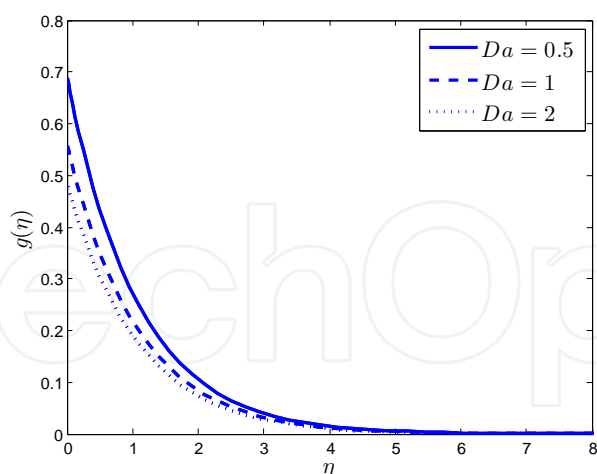
**Figure 15.** The effect of $Da$ on $g(\eta)$ when $K = 0.2; \alpha = 0.5; Grt = 1; Mm = 1; Grm = 1; Pr = 5; R = 1; e = 0.01; Ec = 1; Sc = 1; n = 0.5.$

## 5. Conclusion

Numerical analysis has been carried out in this chapter to study mixed convection heat and mass transfer in MHD flow past a stretching sheet in a micropolar fluid saturated medium under the influence of Ohmic heating. The governing partial differential equations which describe the problem are transformed in a system of ordinary differential equations by using suitable similarity transformations. A recently developed iterative technique together with Chebyshev spectral collocation method is used to solve the highly non-linear and coupled ordinary differential equations. The effects of various physical parameters on the velocity, microrotation, temperature and concentration are obtained. The following main conclusions can be drawn from the present study:

1. The fluid velocity increases with increase in the Grashof numbers, but decreases with increasing values of the Hartman number, local inertia coefficient parameter and inverse Darcy number.

2. The microrotation profiles decrease with thermal/solutal buoyancy force, and the Darcy number, whereas opposite trends are seen by enhancing values of the magnetic field and inertia coefficient parameter.

3. The fluid temperature increases with increasing values of magnetic field, inertia coefficient parameter, while opposite effects are seen by enhancing buoyancy forces and Darcy number.

4. Concentration decreases with increasing values of buoyancy forces and the Darcy number, whereas reverse trends are seen with increasing values of magnetic field, inertia coefficient parameter.

## Acknowledgement

## Author details

Sandile S. Motsa[1] and Stanford Shateyi[2]

1 University of KwaZulu-Natal, South Africa
2 University of Venda, South Africa

## References

[1] D. A. S. Rees, and A. P. Bassom, The Blasius Boundary Layer Flow of a Micropolar Fluid, Int. J. Eng. Sci. 34, 113-124 (1996).

[2] A. Raptis, Flow of a Micropolar Fluid Past a Continuously Moving Plate by the Presence of Radiation, Int. J. Heat Mass Transf. 41, 2865–2866 (1998).

[3] S. Rawat, R. Bhargava and O. A. Bt′eg, A Finite Element Study of the Transport Phenomena in MHD Micropolar Flow in a Darcy-Forchheimer Porous Medium, Proc. WCECS, San Francisco, CA (2007).

[4] S.S. Motsa, New algorithm for solving non-linear BVPs in heat transfer, International Journal of Modeling, Simulation & Scientific Computing, 2:3, 355–373, (2011)

[5] Motsa,S.S.,Sibanda,P. (2012). A linearisation method for non-linear singular boundary value problems, Computers and Mathematics with Applications, 63,1197–1203 (2012)

[6] S.S Motsa,S. Shateyi and P. Sibanda, A Model of Steady Viscous Flow of a Micropolar Fluid Driven by Injection or Suction Between a Porous Disk and a Non-Porous Disk Using a Novel Numerical Technique, Can. J. Chem. Eng. 88:991–1002, (2010).

[7] D. Pal and S. Chatterjee, Mixed convection magnetohydrodynamic heat and mass transfer past a stretching surface in a micropolar fluid-saturated porous medium under the influence of Ohmic heating, Soret and Dufour, Comm. Nonlinear Sci. Numer. Simul. 16, 1329-1346, (2011).

[8] D. Pal, Heat and mass transfer in stagnation-point flow towards in a stretching surface in the presence of buoyancy force and thermal radiation, Meccanica, 44,145-158, (2009).

[9] Pal, D., and Mondal, H, The influence of thermal radiation on hydromagnetic Darcy-Forchheimer mixed convection flow past a stretching sheet embedded in a porous medium, Meccanica, 45(2), doi 10.1007/s11012- 010-9334-8, (2010).

[10] S. Shateyi , Motsa S.S,Thermal Radiation Effects on Heat and Mass Transfer over an Unsteady Stretching Surface, Mathematical Problems in Engineering Volume 2009, Article ID 965603, 13 pages doi:10.1155/2009/965603.

[11] S. Shateyi, and Motsa, S. S. Hydromagnetic non-Darcy flow, heat and mass transfer over a stretching sheet in the presence of thermal radiation and Ohmic dissipation. The Canadian Journal of Chemical Engineering, 89: n/a. doi: 10.1002/cjce.20499,(2011).

[12] C. Canuto, M.Y. Hussaini, A. Quarteroni, and T.A. Zang, Spectral Methods in fluid dynamics, Springer-Verlag, Berlin, 1988.

[13] L. N. Trefethen, Spectral Methods in MATLAB, SIAM, 2000.